

A turning point analysis of the ergodic dynamics of iterative maps

P.Schmelcher and F.K.Diakonos
Theoretische Chemie
Physikalisch-Chemisches Institut
Im Neuenheimer Feld 253
69120 Heidelberg
Federal Republic of Germany

July 3, 2018

Abstract

The dynamics of one dimensional iterative maps in the regime of fully developed chaos is studied in detail. Motivated by the observation of dynamical structures around the unstable fixed point we introduce the geometrical concept of a turning point which represents a local minimum or maximum of the trajectory. Following we investigate the highly organized and structured distribution of turning points. The turning point dynamics is discussed and the corresponding turning point map which possesses an appealing asymptotic scaling property is investigated. Strong correlations are shown to exist for the turning point trajectories which contain the information of the fixed points as well as the stability coefficients of the dynamical system. For the more specialized case of symmetric maps which possess a symmetric density we derive universal statistical properties of the corresponding turning point dynamics. Using the turning point concept we finally develop a method for the analysis of (one dimensional) time series.

1 Introduction

In the past twenty years one dimensional iterative maps have attracted much attention and became a very active field of research. An important reason for the strong interest in the dynamics generated by iterative maps is the fact that they exhibit a variety of typical nonlinear phenomena such as period multiplication, intermittency and chaotic behaviour [Grossmann and Thomae, 1977, Feigenbaum, 1978, Feigenbaum, 1979, Collet and Eckmann, 1980, Crutchfield et al, 1982, Ott, 1993, Schuster, 1994]. They provide therefore a tool for the modeling and simulation of the dynamics of more complicated systems as they typically occur in physics, chemistry and biology. In particular the chaotic dynamics has by now been shown to be of potential importance in many different fields like for example fluids [Gollub and Benson, 1980], plasmas [Sagdeev et al, 1990], circuits [Linsay, 1981] and lasers [Arecchi et al, 1982]. Many of the characteristic features observed in dissipative systems of higher dimensional phase space have their origin in the universal behaviour of one dimensional processes.

Of particular relevance are the maps of the unit interval which possess a single smooth maximum. Due to their noninvertibility they show a very rich behaviour when a control parameter is changed continuously. A typical phenomenon is the bifurcation route to chaos and its universal scaling laws which have been studied in detail in the literature [Grossmann and Thomae, 1977, Feigenbaum, 1978, Collet and Eckmann, 1980] and are now well understood. This bifurcation route leads to an attractor which is, with further changing control parameter, followed by an inverse band bifurcation and ends up in the final state of fully developed chaos. It is the purpose of the present paper to investigate the dynamics of these maps for fully developed chaos, i.e. in their chaotic and ergodic state. Common quantities describing this state are the Ljapunov exponent λ which yields the rate of exponential divergence for neighbouring trajectories and the invariant density ρ which is a measure for the distribution of orbits in the ergodic limit. For further characterization one can use the non-uniformity factor which measures the deviation of the rate of divergence from its average or the correlation function [Györgyi and Szeffalussy, 1984]. Our investigation is aimed at a further understanding of the state of fully developed chaos and goes beyond the above quantities [Diakonov and Schmelcher, 1997]. This will provide us valuable insights into the underlying structure of the ergodic dynamics of maps. We emphasize that

the turning point properties and concepts developed in the present paper are valid for any one dimensional smooth and single humped map for which the rank two image of the extremum merges into an unstable fixed point with a positive multiplier. We shall call this rather general class of maps in the following SSH maps. The only exception is the universal statistical behaviour derived in Sec.5 which holds only for doubly symmetric maps, i.e. for symmetric maps which possess a symmetric density.

In detail we proceed as follows. In chapter 2 we begin by illustrating some eye-catching features of a typical one dimensional ergodic trajectory. These features do *not* show up in the invariant density but are related to the distribution of the oscillations of the trajectories. We also introduce in chapter 2 the concept of turning points and discuss the role of turning points in the ergodic dynamics. A comparison of the chaotic map with a random map with the same invariant density clearly reveals the structures embedded in the fully chaotic and ergodic dynamics. In chapter 3 the turning point map (TPM) is introduced and analyzed. It possesses an important scaling behaviour which develops by joining together humps of successive iterates of the original map. Chapter 4 is devoted to a turning point analysis of higher iterates of the map. Important dynamical information is shown to be present in these higher TPMs. In particular higher periodic orbits, their preimages as well as local stability coefficients are exhibited in the TPMs. Chapter 5 contains a derivation of the universal statistical turning point properties for doubly symmetric maps. In chapter 6 we use our turning point concept in order to develop a method for the analysis of one dimensional time series. Chapter 7 concludes with a summary.

2 The dynamics and the distribution of turning points

In the ergodic case of fully developed chaotic dynamics the measure of the chaotic trajectories is equal to one. Unstable periodic orbits are dense in this chaotic 'sea' but they are of measure zero. Let us begin our investigation by considering a typical chaotic trajectory. For reasons of illustration we hereby choose the logistic map in the ergodic limit $x(n+1) = 4x(n)(1-x(n))$. We emphasize however that our main observations and results of investigations

are valid for any SSH map. Figure 1 shows such an ergodic trajectory for 1.5×10^4 iterations together with its invariant density for 10^6 iterations. The invariant density of the logistic map is given by $\rho_L = \frac{1}{\pi\sqrt{x(1-x)}}$. Both its smoothness in the open interval $]0, 1[$ as well as its singular behaviour at $x = 0, 1$ can clearly be seen in the density of the trajectory given in Fig.1.

A closer look at the trajectory itself in Fig.1 gives us the impression that there exists a dynamical structure in the neighbourhood of $x_F = \frac{3}{4}$ which is the position of the unstable fixed point (x_F refers in the following always to the fixed point different from zero of the map). This structure possesses no counterpart in the corresponding smooth invariant density $\rho_L(x)$. Figure 2 shows the trajectory for fewer iterations which reveals that the above-mentioned structure in the neighbourhood of the fixed point might have its origin in the nonuniform distribution of oscillations in the interval $[0, 1]$: we observe an enhanced probability for finding small amplitude oscillations in the vicinity of the fixed points. Before investigating these properties in more detail let us introduce the following notions: a turning point $x(n)$ of a trajectory (abbreviated by *TP*) is a point which represents a local maximum or minimum of the trajectory (see Eq.(1) below for a quantitative criterion for the turning point). We remark that the name 'turning point' should not be confused with the same name that often refers to the local extrema of a map f . The center of oscillations (abbreviated by *CO*) are defined to be the midpoints between subsequent local maxima and minima (and vice versa) and the abbreviation *AO* means the amplitude of the corresponding oscillations.

In the following we analyze the dynamical properties of the turning points. This will lead us to a qualitative as well as quantitative understanding of the mechanisms which create, among others, the corresponding structures (see below) in the relevant densities. We begin by deriving a necessary and sufficient condition so that a point $x(n)$ of an ergodic trajectory is a turning point. Our starting point is the geometric condition

$$(x(n+1) - x(n)) \times (x(n) - x(n-1)) < 0 \quad (1)$$

for a turning point $x(n)$ where $x(n+1) = f(x(n))$ and f is a single humped and smooth map. x_1 is the inverse image of the fixed point x_F on the left branch $[0, x_m]$ of the map f where x_m is the maximum of the map f . We will show in the following that given a map f and its fixed point x_F the

condition for $x(n)$ to become a turning point is $x(n-1) > x_1$. Since the map f is monotonically increasing on $[0, x_m]$ and decreasing on $[x_m, 1]$ we have to distinguish three cases. For $x(n-1) < x_1$ we obtain the inequality $x(n-1) < x(n) < x(n+1)$ and therefore $x(n)$ is not a turning point. In contrast to this we obtain for $x(n-1) \in [x_1, x_F]$ the inequalities $x(n-1) < x(n)$ and $x(n) > x(n+1)$ and $x(n)$ is a turning point. The third case is $x(n-1) \in [x_F, 1]$ which yields $x(n-1) > x(n)$ and $x(n+1) > x(n)$, i.e. $x(n)$ is a turning point. In total we therefore arrive at the condition $x(n-1) > x_1$ for $x(n)$ to become a turning point. Otherwise, i.e. for $x(n-1) < x_1$, $x(n)$ is a non turning point. For the special case of the logistic map this means $x(n-1)$ has to be larger than $\frac{1}{4}$ in order for $x(n)$ to become a turning point.

With this result we are now able to understand and discuss the occurrence of turning points, i.e. we gain insights into the dynamics of turning points. (see in particular also Fig.2 for an illustration of the turning point dynamics). In the following we distinguish between different phases of the motion created by the iterations of the map. Successive iterations of the map which are located in the interval $[0, x_1]$ belong to a stretching phase of the iterative motion. Apart from the very first point (see below) in the interval $[0, x_1]$ the points $x(n)$ of this phase obey $x(n-1) < x_1$ and are therefore non turning points. Once we leave the interval $[0, x_1]$ the first point $x > x_1$ obeys $x \in [x_1, x_F]$ and is also a non turning point. The next series of iterated points obey alternately $x > x_F > x_1$ and $x_1 < x < x_F$ and we therefore obtain an oscillating stretching phase of motion around the fixed point x_F which consists exclusively of turning points. These stretching phases end in case we obtain $x > x^*$ where x^* is the inverse image of x_1 on the right branch $[x_m, 1]$ of the map f (for the logistic map we have $x^* = \frac{3}{4} + \frac{1}{4}(\sqrt{3} - 1)$). The next iterated point x is then folded back into $[0, x_1]$ and represents a turning point. Subsequently the next stretching phase of non turning points in the interval $[0, x_1]$ starts etc. Both the stretching phase as well as the oscillatory phase of motion can nicely be seen in Figure 2.

In order to gain further insights into relevant turning point properties we have illustrated in Fig.3 the density ρ_{TP} of the turning points for a typical chaotic trajectory of the logistic map. First of all we realize that ρ_{TP} exhibits a step like structure at the position x_F of the unstable fixed point. We observe an enhanced probability of finding turning points in the interval $[x_F, 1]$. The singular behaviour of the turning point density at $x = 0$ and $x = 1$ is, apart from a constant factor, the same as that for the density ρ_L and characteristic

for the underlying dynamical law.

It is possible to understand the origin of the step-like structure of the turning point density ρ_{TP} in Fig.3 analytically. Using the above condition $x(n-1) > x_1$ for $x(n)$ to become a turning point we obtain the density of the preimages of the turning points: $\mathcal{N}\rho_L(x)\Theta(x-x_1)$. Here Θ is the step function $\Theta(x) = \{1 \text{ for } x > 0; 0 \text{ for } x < 0\}$ and \mathcal{N} the corresponding normalization constant. Mapping this density forward with f we get the expression $\frac{\mathcal{N}}{2}\rho_L(x)(1+\Theta(x-x_F))$ for the density of the turning points. This short derivation clearly shows that the step like structure of the turning point density at the position of the fixed point is a common property for all SSH maps. Looking at the turning point density therefore immediately reveals the positions of the fixed points different from zero for a given SSH map.

In order to get an impression of the dynamical information contained in Fig.3 we have to compare the turning point density ρ_{TP} of the logistic map with the density of turning points ρ_{RTP} which is generated by the weighted random map. (The weighted random map is chosen to possess the same density as the chaotic map, i.e. $\rho_R = \rho_L$).

Indeed the density ρ_{RTP} can be derived in closed form via the following considerations. Given the tent map $g(y) = \{2y \text{ for } y \leq \frac{1}{2}; (2-2y) \text{ if } y \geq \frac{1}{2}\}$ it is well-known that the conjugacy between g and the logistic map f is given by the homeomorphism $h(y) = \frac{1-\cos(\pi y)}{2}$, i.e. $h \circ g = f \circ h$. The invariant density of g is equal to one on the whole unit interval. If $y(n) = y$ is a point of the interval, the probability that it is a turning point is $y^2 + (1-y)^2$. The normalized random turning point distribution σ_{RTP} belonging to the random map with unit density, i.e. $\sigma_R = 1$, is therefore given by $\sigma_{RTP} = \frac{3}{2}[y^2 + (1-y)^2]$. The enhancement of the turning point density σ_{RTP} compared to σ_R at 0 and 1 are geometric boundary effects. Since the conjugacy h preserves the turning points and transports the invariant density for g to the invariant density of f we can treat the application of h as a coordinate change of the unit interval. As a result the weighted random turning point density ρ_{RTP} takes on the following appearance

$$\rho_{RTP}(x) = \frac{\sigma_{RTP}(y)}{\pi\sqrt{x(1-x)}} = \frac{6[(\arcsin\sqrt{x})^2 + (\arccos\sqrt{x})^2]}{\pi^3\sqrt{x(1-x)}} \quad (2)$$

ρ_{RTP} is symmetric with respect to $\frac{1}{2}$ and smoothly monotonically decreasing and increasing in $]0, \frac{1}{2}[$ and $[\frac{1}{2}, 1[$, respectively. It possesses power singularities

at $x = 0$ and $x = 1$ which are apart from a constant factor the same as for ρ_R .

To investigate this further we have illustrated in Fig.4a the density for the centers of the oscillations ρ_{LCO} and in Fig.4b the density for the amplitudes of the oscillations ρ_{LAO} for the trajectory of the logistic map shown in Figs.1/2. First of all we observe that the density ρ_{LCO} is nonzero only in a subset of the unit interval, namely for approximately $x \in [0.38, 0.78]$. The density for the centers of the oscillations shows three main peaks. The largest peak is located at $\frac{1}{2}$. Two other major peaks are located at approximately 0.58 and 0.78, respectively. The centers of the oscillations are therefore not smoothly distributed but exhibit certain dynamically preferred values. In addition the density ρ_{LCO} shows a number of small dips and step like structures. The density for the amplitudes of the oscillations shown in Fig.4b exhibits a progression of four sharp peaks which are preceded by step like and strongly ascending broad structures. The positions of the peaks are approximately 0.56, 0.86, 0.96 and 1.0, respectively, which represent the dynamically preferred amplitudes of the oscillations. Both the distribution ρ_{LCO} of the centers as well as the density ρ_{LAO} for the amplitudes of the oscillations of the trajectories contain therefore dynamical information which is in particular responsible for the above-observed structures in the trajectory. We emphasize that looking at both ρ_{LCO}, ρ_{LAO} with increasing resolution reveals an increasing number of structures and detailed properties. Part of these structures can be derived analytically by the following considerations.

Consider the points $x_0 = 1$ and $x_k = (f|_{[0, \frac{1}{2}]})^{-k}(x_F)$ for $k > 0$ which are the preimages of the fixed point on the left branch of the map f . If the point $x(n) = x$ is a turning point and $x \in (x_k, x_{k-1}]$ then the next turning point is $x(n+k) = f^k(x)$. Set

$$\varphi_k(x) = \frac{f^k(x) + x}{2} \quad (3)$$

which defines the center of an oscillation. Then

$$\rho_{LCO} = \sum_{k=1}^{\infty} (\varphi_k)_* (\rho_{TP} \chi_{(x_k, x_{k-1}]}) \quad (4)$$

where χ_A denotes the characteristic function of A (1 on A and 0 outside A). The Perron-Frobenius operator $(\varphi_k)_*$ transforms the densities in the usual

way

$$((\varphi_k)_*(\rho))(x) = \sum_{\varphi_k(y)=x} \frac{\rho(y)}{|\varphi'_k(y)|} \quad (5)$$

In particular, the support of ρ_{LCO} is the union of the supports of the densities $(\varphi_k)_*(\rho_{TP\chi(x_k, x_{k-1})})$, that is the union of the sets $(\varphi_k)((x_k, x_{k-1}])$. We have therefore for the logistic map

$$\varphi_1(x) = \frac{5x - 4x^2}{2} \quad (6)$$

and $(x_0, x_1] = (\frac{1}{4}, 1]$. The critical point, i.e. maximum, of φ_1 is $\frac{5}{8}$. In addition $\varphi_1(\frac{1}{4}) = \frac{1}{2}$, $\varphi_1(\frac{5}{8}) = \frac{25}{32}$, and $\varphi_1(1) = \frac{1}{2}$. Therefore $\varphi_1((x_1, x_0]) = [\frac{1}{2}, \frac{25}{32}]$.

If $k > 1$ and $x \in (x_k, x_{k-1}]$ then $f^{k-1}(x) \in (x_1, x_F]$ and $f^{k-1} > x$ so

$$\varphi_k(x) = \frac{f^k(x) + x}{2} < \frac{f^k(x) + f^{k-1}(x)}{2} = \varphi_1(f^{k-1}(x)) \leq \frac{25}{32} \quad (7)$$

On the other hand, $f^k(x) \in [x_F, 1]$, so

$$\varphi_k(x) = \frac{f^k(x) + x}{2} > \frac{f^k(x)}{2} \geq \frac{x_F}{2} = \frac{3}{8} \quad (8)$$

Therefore the support of ρ_{LCO} is contained in $[\frac{3}{8}, \frac{25}{32}]$. Moreover, for $k > 1$ there are points $a_k, b_k \in (x_k, x_{k-1}]$ with $f^k(a_k) = x_F$ and $f^k(b_k) = 1$. We have

$$\left[\frac{a_k + x_F}{2}, \frac{b_k + 1}{2} \right] \subset \varphi_k((x_k, x_{k-1}]) \quad (9)$$

and $\frac{(a_k + x_F)}{2} \leq \frac{(x_{k-1} + x_F)}{2}$, $\frac{b_k + 1}{2} > \frac{1}{2}$, so

$$\left[\frac{x_{k-1} + x_F}{2}, \frac{1}{2} \right] \subset \varphi_k((x_k, x_{k-1}]) \quad (10)$$

Therefore the support of ρ_{LCO} is equal to $[\frac{3}{8}, \frac{25}{32}]$.

Apart from the support of the quantity ρ_{LCO} also its singularity structure can be derived. ρ_{LCO} possesses singularities whenever ρ_{TP} has a singularity or φ'_k is zero. There are two singularities of ρ_{TP} : at 0 and 1. The singularity at 1 gets carried by $(\varphi_1)_*$ to $\frac{1}{2}$, so ρ_{LCO} has a singularity at $\frac{1}{2}$. The singularity at 0 gets "washed out", since as $k \rightarrow \infty$, the derivative of φ_k is of order 2^k , whereas

ρ_{TP} on $(x_k, x_{k-1}]$ is only of order 2^{-k} . However, the zeros of φ'_k produce additional singularities of ρ_{LCO} (one singularity for every k). In particular, $\varphi'_1(\frac{5}{8}) = 0$, so we get a singularity of ρ_{LCO} at $\frac{25}{32}$. For $k = 2$ we have $\varphi'_2(t) = 0$ for $t \approx 0.163$ (t is a solution to $256t^3 - 384t^2 + 160t - 17 = 0$) and we get a singularity of ρ_{LCO} at $\varphi_2(t) \approx 0.577$. To summarize, the distribution for the center of oscillations ρ_{LCO} possesses a highly nontrivial structure on a finite subset of the unit interval and shows in particular infinitely many singularities which reflect the fact that the infinitesimal turning point neighbourhood of the origin 0 is mapped to arbitrary detail to the turning points in the finite neighbourhood of the fixed point x_F (see below in the context of the turning point map).

To make the structures contained in the ergodic chaotic dynamics even clearer we have illustrated in Fig.5a and 5b the corresponding densities ρ_{RCO} and ρ_{RAO} for a weighted random map which possesses the same density $\rho_R = \rho_L$ as the logistic map. The density for the centers of the oscillations ρ_{RCO} of the random map exhibits a single broad peak which is centered around $\frac{1}{2}$ and decays monotonically towards the boundaries of the unit interval. The most probable value for the position of the center of the oscillations is therefore $\frac{1}{2}$ and the probability for values different from $\frac{1}{2}$ decreases with increasing distance of the corresponding value from $\frac{1}{2}$. In comparison with the density ρ_{LCO} (see Fig.4a) of the logistic map whose origin is a dynamical law the density ρ_{RCO} belonging to the random map shows a very simple and smooth structure. Figure 5b shows the density ρ_{RAO} for the amplitudes of the oscillations for the same weighted random map. ρ_{RAO} is monotonically increasing on the unit interval with a strongly peaked maximum at $x = 1$. Within the statistical accuracy of Fig.5b ρ_{RAO} is a smooth distribution without any structures. This clearly reveals that the fully chaotic system contains dynamical information according to the distributions ρ_{LCO} and ρ_{LAO} which is not present in the corresponding distributions ρ_{RCO} and ρ_{RAO} of the random map.

To complete our picture of the oscillatory motion of the random map on the one hand and of a 1D dynamical law on the other hand we have illustrated in Fig.6 the occupied coordinate space for the amplitudes of the oscillations as a function of the center of the oscillations for both the weighted random map $x_{RAO}(x_{RCO})$ in Fig.6a as well as the logistic map $x_{LAO}(x_{LCO})$ in Fig.6b. For the case of the random map, $x_{RAO}(x_{RCO})$ fills the two-dimensional area

of an isosceles triangle (see Fig.6a). In contrast to this the corresponding quantity $x_{LAO}(x_{LCO})$ for the logistic map is a one dimensional curve (see Fig.6b) which consists, apart from a cross diagonal line, of a series of skew and increasingly peaked humps. With increasing absolute values of these humps their widths tend to zero, i.e. the series of humps approaches an accumulation line which is the limiting line of the upper left part of the curve shown in Fig.6b. Again it is obvious that there exists a major difference between the 'motion' of the random map which is distributed according to its weight and the highly organized motion of the logistic map which shows according to Fig.6b a number of interesting structures.

We emphasize that the above-observed properties and behaviour of the oscillatory motion of maps are by no means restricted to our specific example, namely the logistic map: all SSH maps show a very similar behaviour. This includes the special family of symmetric beta maps which has been introduced recently [Diakonov and Schmelcher, 1996] and possesses members with a wide range for the order of the maximum and for the singular behaviour of the densities at the positions $x = 0, 1$.

Let us now investigate how subsequent turning points are mapped onto each other.

3 The turning point map and its scaling properties

Having discussed the occurrence of turning points in the dynamics of the map f we introduce now the turning point map (TPM), i.e. the map of a turning point onto its subsequent turning point. The TPM will be a key quantity for our understanding of the structures and organization in the ergodic dynamics of iterative maps. Figure 7 shows the TPM belonging to the logistic map on a logarithmic scale. For reasons of illustration we have chosen the logistic map as a specific example. However, as already emphasized our arguments are valid for any SSH map. The monotonous part of the TPM for $x_F < x(n) < 1$ has its origin in the fact that the turning points in the interval $[x_F, 1]$ are mapped via the TPM onto the interval $[0, x_F]$. The first hump in Fig.7 represents the image of the interval $[x_1, x_F]$ with respect to the TPM. Since turning points in the interval $[x_1, 1]$ are mapped directly onto turning points

by the map f itself the TPM in $[x_1, 1]$ simply reflects the shape of f in this interval.

The eye-catching feature of the TPM for $x < x_1$ is the extreme similarity of its subsequent humps with decreasing values of $x(n)$ on a logarithmic scale. Approaching smaller and smaller values for $x(n)$ Fig.7 suggests an asymptotically exact scaling law for subsequent humps. The TPM possesses an accumulation point of its humps at the origin and has dimension 1. For values $x < x_1$ the TPM shows us how turning points in the neighbourhood of the origin $U_\epsilon(0)$ (which have their preimage in the neighbourhood $U_\delta(1)$ of 1) are mapped onto the turning points in the finite interval $[x_F, 1]$. The TPM does this according to Fig.7 to arbitrary detail and in a self repeating form if we approach the origin.

As indicated in Fig.7 the vertical positions on the axis $x(n+1)$ of the turning points $\{x_i\} = (x_1, x_2, x_3, x_4, \dots)$ of the TPM are all the same and given by the fixed point x_F . The horizontal positions of these turning points on the axis labeled $x(n)$ are the positions of successive preimages of the fixed point x_F on the left branch of the map f . The abscissae of x_1 is therefore the preimage $f^{-1}(x_F)$ of the fixed point x_F in the interval $[0, x_m]$, the abscissae of x_2 is the preimage $f^{-1}(x_1)$ of x_1 in the interval $[0, x_m]$, etc... This series of preimages obviously converges towards the unstable fixed point 0 and the ratio of subsequent preimages converges towards the derivative of the map f at the origin, i.e. we have

$$\kappa = f'(0) = \lim_{i \rightarrow \infty} \frac{x_{i+1}}{x_i} \quad (11)$$

For the special case of the logistic map we have $x_i = \frac{1}{2}(1 - \frac{1}{2}\sqrt{2 + \sqrt{2 + \dots \sqrt{2 + \sqrt{3}}}})$ with $i - 1$ nested roots.

But not 'only' the turning points of the TPM $\{x_i\}$ scale asymptotically with a factor κ but in particular also successive humps defined in the intervals $\Delta_i = [x_{i+1}, x_i]$ converge asymptotically with the same ratio against a final shape. A numerical as well as analytical closer investigation of the i -th hump of the TPM in the interval Δ_i reveals that it is identical to the top of the first hump of the i -th iterate f^i of the map f . More precisely: the i -th hump of the TPM is identical to the intersection $x(n+1) > x_F$ of f^i which is closest to the unstable fixed point 0. Putting everything together the TPM is given

by

$$f_{tp} = f^{i+1}(x) \quad \forall x \in \Delta_i, \quad \forall i \geq 0 \quad (12)$$

with $\Delta_0 = [x_1, 1]$. Approaching the origin the TPM can therefore be considered as a sequence of the top of the humps of higher and higher iterated maps. We remark that even the position of the humps of the TPM is the same as for the corresponding iterates f^i .

In addition the series of humps of the TPM converges, apart from the scaling, against an asymptotic final shape. This asymptotic form can be obtained by using the scaling property of the humps $f^{n+1}(x) = f^n(\delta_n x)$ which are now defined on the interval $0 \leq x \leq s_{n+1}$ with s_{n+1} being the first zero, i.e. the zero closest to the origin, of the iterate f^n . $\delta_n = \frac{s_n}{s_{n+1}}$ is the ratio of the first zeros of successive iterates of the map f . Introducing a new rescaled variable $z = \frac{x}{s_{n+1}}$ which is defined on the whole unit interval the renormalized asymptotic functional form of the complete first hump is given by

$$h(z) = \lim_{n \rightarrow \infty} f^n(z s_n) \quad (13)$$

This equation provides a method for the systematic approximation of the asymptotic form $h(z)$ by calculating successive iterates of the map as well as their first zeros. The convergence properties of this procedure turn out to be excellent.

Having understood much of the dynamics of the turning points and in particular the structure of the turning point map we turn now to the question of the correlation of the dynamics of the turning points. It is well-known [Györgyi and Szepfalusy, 1984] that the strongest decay of the correlation function occurs for the ergodic limit of the doubly symmetric maps. They possess δ -correlated processes, i.e. their subsequent steps are completely uncorrelated. Using the common definition of the correlation function $C_f(n) = \langle (x - \langle x \rangle_f)(f^n(x) - \langle x \rangle_f) \rangle_f$ this means $C_f(n) = C_f(0)\delta_{n0}$. Fig.8 shows now the absolute value of the correlation function of the dynamics of the turning points in comparison with the corresponding correlation function of a typical ergodic trajectory for the case of the logistic map. As expected the correlation function of the chaotic trajectory decays completely with the first time step. (For a non doubly symmetric map the generic decay behaviour can be much 'slower'). In contrast to this, however, the correlation function of the turning points shows only within the first two steps a minor decay and stays subsequently **constant** ! This reveals that the turning points obey a

highly correlated dynamics with infinite correlation length thereby suggesting the interpretation of the turning points as a constituent (phase) of the dynamics which is at a critical point of a phase transition [Beck and Schlögl, 1993].

Let us briefly summarize and comment on our previous results. Our investigation and discussion of the turning point dynamics, the turning point map as well as the correlation function clearly show that a turning point analysis extracts valuable dynamical information from a given ergodic and fully chaotic system. The TPM contains details of the iterates f^i for all i and maps in particular arbitrarily small intervals in the neighbourhood of the origin onto the finite interval $[x_F, 1]$. It obeys an asymptotic scaling law and converges to a repeating functional form which can be derived according to the above-given construction scheme. The fixed points as well as its preimages x_F (see in particular also chapter 4 which provides an investigation of the turning point maps for higher iterates of the map f) play hereby a particularly important role. The turning point dynamics shows an infinite correlation length of the corresponding correlation function, i.e. the turning point analysis extracts the correlated part from the original trajectory. The origin of this strong correlation is the oscillating dynamics around the fixed point x_F .

In extension of the construction scheme for the TPM it is possible to define so-called renormalized limit functions which are the sequence of suitably scaled humps of the infinitely high iterates of the map f . These limit functions include not only the first hump (see Eq.(13)) but all oscillations of the infinitely high iterates $\lim_{n \rightarrow \infty} f^n$ of the original map f . To achieve this we define

$$f_k^n(z) = f^n((r_k^{(n)} - r_{k-1}^{(n)})z + r_{k-1}^{(n)}) \quad \text{for } z \in [0, 1] \quad (14)$$

where $r_k^{(n)}$ is the k -th zero of the corresponding iterate f^n . Equation (14) scales neighbouring zeros which converge to the same value with increasing iterations to the unit interval. The desired renormalized family of limit functions $g^{(k)}(z)$ which describe the humps between the zeros $r_{k-1}^{(n)}$ and $r_k^{(n)}$ for $n \rightarrow \infty$, i.e. of the infinitely high iterate of f , is then given by the limit process

$$g^{(k)}(z) = \lim_{n \rightarrow \infty} f^n((r_k^{(n)} - r_{k-1}^{(n)})z + r_{k-1}^{(n)}) \quad \text{for } z \in [0, 1] \quad (15)$$

Let us illustrate the above procedure for the example of the logistic map in

the ergodic limit. The n -th iteration $x(n)$ of a point $x(0)$ can for this case be given analytically [Pincherle, 1920, Kadanoff, 1983]

$$x(n) = \frac{1}{2} [1 - \cos(2^n \arccos(1 - 2x(0)))] \quad (16)$$

The zeros $r_k^{(n)}$ take on the following appearance

$$r_k^{(n)} = \frac{1}{2} \left[1 - \cos \left(\frac{k\pi}{2^{n-1}} \right) \right] \quad (17)$$

Applying the renormalization and limiting procedure according to Eq.(15) the following result for the limit function $g_L^{(k)}(z)$ of the logistic map can be derived

$$g_L^{(k)}(z) = \frac{1}{2} \left[1 - \cos \left(2\pi \sqrt{(k-1)^2 + (2k-1)z} \right) \right] \quad \text{for } k = 1, 2, \dots \text{ and } z \in [0, 1] \quad (18)$$

The next chapter is devoted to a turning point analysis of doubly iterated maps f^2 and will give us a general idea of the information contained in arbitrarily high iterates f^n .

4 Dynamical information of the turning point maps for higher iterates of the map

Let us begin our investigation of the TPMs belonging to higher iterates f^i by deriving the general turning point criterion. According to Eq.(1) turning points occur if

$$\mathcal{A}(x(n-1)) = (F(F(x(n-1))) - F(x(n-1))) \times (F(x(n-1)) - x(n-1)) < 0 \quad (19)$$

where $F = f^i$ can now be any iterate of the original map f . In order to determine the transition from turning points to non-turning points or vice versa in the criterion Eq.(19) we have to look for those zeros $x(n-1)$ of \mathcal{A} for which \mathcal{A} changes from positive to negative values or vice versa, i.e. the zeros with $\frac{\partial \mathcal{A}}{\partial x}(x(n-1)) \neq 0$. If $x(n-1)$ is a fixed point we have both $\mathcal{A}(x(n-1)) = 0$ and $\frac{\partial \mathcal{A}}{\partial x}(x(n-1)) = 0$ and $x(n-1)$ is not a point which separates turning points from non turning points with respect to $x(n) = F(x(n-1))$. However,

if $x(n-1)$ is the preimage p_i of a fixed point and consequently $x(n)$ a fixed point we obtain $\mathcal{A}(x(n-1)) = 0$ and in particular

$$\frac{\partial \mathcal{A}}{\partial x}(x(n-1)) = (x(n-1) - x(n)) \times F'(x(n-1)) \times (1 - F'(x(n))) \neq 0 \quad (20)$$

since $|F'(x(n))| > 1$ (we have only unstable fixed points) and we consider only those preimages of the fixed points which possess a derivative $F'(x(n-1)) \neq 0$. This means that the preimages of the fixed points determine the transition points from turning points to non turning points or vice versa. We therefore obtain the following turning point criterion. The preimages $\{p_i\}$ of the fixed points define a unique partitioning of the unit interval $[0, 1]$ into subintervals $I_i = [p_i, p_{i+1}]$. In order for $x(n)$ to become a turning point $x(n-1)$ has to obey the necessary and sufficient condition $x(n-1) \in \cup_{i=0}^l I_{2i+1}$.

Let us illustrate this for the example of the twice iterated logistic map $F = f^2$. f^2 possesses four fixed points, namely $\{x_{F_i}\} = \{0, \frac{5-\sqrt{5}}{8}, \frac{5+\sqrt{5}}{8}, \frac{3}{4}\}$ with alternating positive and negative derivatives $f^{2'}(x_{F_i})$, respectively. The preimages of the fixed points which obey the above condition $F'(p_i) \neq 0$ are

$$\begin{aligned} p_1 &= \left(\frac{1}{2} - \frac{1}{2}\sqrt{\frac{5+\sqrt{5}}{8}}\right) & p_2 &= \frac{1}{2}\left(1 - \frac{\sqrt{3}}{2}\right) \\ p_3 &= \frac{1}{2}\left(\frac{3}{4} - \frac{\sqrt{5}}{4}\right) & p_4 &= \left(\frac{1}{2} - \frac{1}{2}\sqrt{\frac{5-\sqrt{5}}{8}}\right) \\ p_5 &= \frac{1}{4} & p_6 &= \frac{1}{2}\left(\frac{3}{4} + \frac{\sqrt{5}}{4}\right) \\ p_7 &= \left(\frac{1}{2} + \frac{1}{2}\sqrt{\frac{5-\sqrt{5}}{8}}\right) & p_8 &= \frac{1}{2}\left(1 + \frac{\sqrt{3}}{2}\right) \\ p_9 &= \left(\frac{1}{2} + \frac{1}{2}\sqrt{\frac{5+\sqrt{5}}{8}}\right) & & \end{aligned} \quad (21)$$

and in addition we have for the first and last point $p_0 = 0$ and $p_{10} = 1$, respectively. $x(n-1)$ has therefore to be located in one of the intervals I_1, I_3, I_5, I_7 or I_9 if we want $x(n)$ to become a turning point.

Before beginning with the discussion of TPM's of higher iterates f^n some remarks are appropriate. There exist two different classes of fixed points for our map f^n . The first class contains the fixed points with a positive derivative, i.e. $f^{n'}(x_{F_i}) > 1$. The local dynamics around these fixed points

can be characterized as an unstable stretching behaviour. The dynamics in the neighbourhood of these points contains no turning points. The second class consists of the fixed points with a negative derivative, i.e. $f^{n'}(x_{Fi}) < -1$. The local dynamics around these fixed points can be characterized as an alternating stretching behaviour which means that successive points are on opposite sides of the corresponding fixed point. Each point of this local dynamics is a turning point. Having these facts in mind we turn now to our discussion of the TPM of doubly iterated maps.

Figure 9 shows the TPM of the doubly iterated logistic map on a logarithmic scale. First of all we observe that there are a number of disconnected objects each of which exhibits a detailed and relatively complicated structure. For $x(n) > y_3$ we observe the objects labeled by (b), (c) and (d) which appear only once. In contrast to this we observe for $x(n) < y_3$ with decreasing values of $x(n)$ a repeating sequence of structures. The absolute unit of these repeating structures consists of two non-overlapping objects which are labeled in Fig.9 by (a) and (e), respectively. Since the repetition of these structures on the logarithmic scale becomes asymptotically exactly periodic we obtain an asymptotic scaling behaviour with respect to the above-mentioned absolute unit consisting of the asymptotic form of the objects (a) and (e). This scaling behaviour is similar to the one observed in the previous chapter for the TPM of the map f itself. The scaling factor is the derivative of the map f^2 at the origin namely $f^{2'}(0)$, i.e. the stability of the fixed point 0. Before entering the discussion of each of the objects (a), (b), (c), (d) separately, we want to extract some important properties from the TPM of the doubly iterated map f^2 which can easily be extended to arbitrary iterates f^i . As indicated in Fig.9 the vertical positions of the lower and upper horizontal edges of the objects (a), (b), (c), (d), (e) etc. are given by the positions of the fixed points $x_{F1}, x_{F2}, x_{F3}, x_{F4}$ and the point 1. The valuable information of the positions of the fixed points can therefore easily be extracted from the corresponding TPM. Higher periodic orbits can simply be localized by extracting the positions of the fixed points from the TPM of higher iterates of the map. In our case of Fig.9 x_{F1} and x_{F3} are fixed points of f whereas $\{x_{F2}, x_{F4}\}$ represents a period two orbit of f .

The TPM of Fig.9 still contains much more information. Let us consider the vertical right and left edges of the individual objects which are part of the TPM. The positions of these edges are indicated in Fig.9 by y_1, y_2, \dots, y_6 . These quantities y_i are the positions of the first or higher preimages of the

fixed point x_{F3} . y_1, y_2, y_3, y_4 are first preimages whereas y_5, y_6 are second preimages of x_{F3} . In general these vertical edges are given by the positions of the preimages of the fixed points with a positive derivative $f^{i'}(x_{Fi}) > 0$. Approaching smaller and smaller values for $x(n)$ we obtain increasingly higher preimages of the corresponding fixed points. After having discussed the positions of the individual objects in the TPM let us now turn to an investigation of the objects themselves.

Apart from the objects of type (e) all constituents of the TPM in Fig.9 consist of a series of humps. The widths of the humps belonging to the objects of type (a) decrease strongly if the values of $x(n)$ approach the corresponding values of the preimages y_i of the fixed point x_{F3} . The objects (b) and (c) possess such an accumulation point of humps only on one side, namely at the position of the preimage y_2 . In order to analyze this series of humps with decreasing widths we have illustrated in Figure 10 important parts of the objects labeled by (a), (b), (c), (d) in Fig.9. Figure 10 (a) shows the object (a) of Fig.9 in the neighbourhood of the preimage y_3 of x_{F3} , i.e. $x(n+1)$ is illustrated as a function of $y_3 - x(n)$ with a logarithmic abscissae.

The eye-catching feature is the asymptotically ($x(n) \rightarrow y_3$) exact scaling behaviour of the individual humps with a constant scaling factor. We therefore encounter not only the above-mentioned scaling behaviour of the series of objects of type (a), (e) but also a scaling behaviour of the interior of the objects themselves (apart from (e)). The corresponding interior scaling factor is in the case of Fig.10 (a) $f^{2'}(x_{F3})$, i.e. the derivative of the map f^2 at the position of the fixed point (x_{F3}) with a positive derivative. The lower turning points δy_{3i} for $i = 1, 2, 3$ indicated in Fig.10 (a) represent a series of increasingly higher preimages of the fixed point x_{F4} which possesses a negative derivative $f^{2'}(x_{F4}) < 0$. This series converges in an asymptotically scaling way towards the preimage y_3 of x_{F3} . The structure of the object (a) can be explained in even more detail. The series of humps can be obtained by intersecting increasingly higher iterates f^{2n} of the map f^2 with the line $x(n+1) = x_{F4}$ and joining together the resulting humps. In this sense the object (a) describes the top $x(n+1) > x_{F4}$ of the humps of arbitrarily high iterates of the map f^2 in the interval $[y_4, y_3]$. Most of the properties discussed for the example of the individual object labeled (a) can also be observed for the other constituents of the TPM in Fig.9.

Figure 10 (b) shows the object labeled (b) in Fig.9 in the neighbourhood of the preimage y_2 , i.e. $x(n+1)$ as a function of $y_2 - x(n)$ with a logarithmic

abscissae. The same asymptotic scaling behaviour now for $x(n) \rightarrow y_2$ can be observed and the scaling factor is again determined by the stability of the fixed point (x_{F3}) which possesses a positive derivative. The upper turning points δY_{2i} for $i = 1, 2, 3$ indicated in Fig.10 (b) represent a series of increasingly higher preimages of the fixed point x_{F2} which possesses a negative derivative $f^{2'}(x_{F2}) < 0$. This series converges in an asymptotically scaling way towards the preimage y_2 of x_{F3} . The series of reversed humps can be obtained by intersecting increasingly higher iterates of the map f^2 with the line $x(n+1) = x_{F2}$ and taking the lower part $x(n+1) < x_{F2}$. Figures 10 (c) and (d) illustrate the structures of the objects (c) and (d) in Fig.9. Asymptotic scaling properties are again observed and described by the stability of the fixed point with a positive derivative. For Fig.10 (c) the lower turning points δy_{2i} for $i = 1, 2, 3$ which represent increasingly higher preimages of the fixed point x_{F4} converge towards the preimage y_2 of the fixed point x_{F3} . The humps of the object (c) can be explained analogously to the humps in Fig.10(a). Finally Fig.10 (d) shows a scaling of reversed humps towards the preimage y_1 and another series of the preimages δy_{1i} of the fixed point x_{F3} which converges to y_1 .

Let us briefly summarize the observations. Turning point maps belonging to higher iterates of the original map f contain a number of dynamically most relevant informations. It is easy to extract the position of not too long periodic orbits, their stability coefficients as well as the (higher) preimages of the fixed points of f by considering the TPM of the corresponding iterate f^n . The TPMs themselves as well as their disconnected constituents show an asymptotic scaling behaviour and exactly describe important parts of arbitrarily high iterates of the map f .

To conclude our discussion of the TPMs of higher iterates f^n we show in Fig.11 the density $\rho_{TP2}(x)$ of turning points for the doubly iterated map f^2 . We observe step like structures at the positions of the fixed points x_{Fi} which reflect the above-discussed properties of the corresponding turning point map. The singular behaviour of $\rho_{TP2}(x)$ at the boundaries of the unit interval is apart from a constant factor the same as for the density of the map itself.

5 Statistical properties of the turning point dynamics

Having studied in detail the dynamical properties of the turning points in the previous chapters we turn now to an investigation of the statistical turning point properties. In contrast to the previous Secs. the results of the present Sec. hold only for doubly symmetric maps. A measure for the frequency of the turning points is given by the ratio of the number of turning points N_{tp} and the total number of points N_{tot} , i.e. $P_{tp} = \frac{N_{tp}}{N_{tot}}$. One half of that number (that is, only minima counted) has been called wave number [Ding, 1988] or over rotation number [Blokh and Misiurewicz] in the literature. Since we are dealing with a fully chaotic and ergodic system the quantity P_{tp} is solely determined by the necessary and sufficient condition $x(n-1) > x_1$ for a turning point $x(n)$ and the frequency with which a certain region of the interval is visited. This frequency is however given by the invariant density $\rho_f(x)$ of the map f . We therefore obtain the following expression for the portion of turning points of the chaotic trajectories

$$P_{tp} = \int_{x_1}^1 \rho_f(x) dx \quad (22)$$

where $x_1 = (1 - x_F)$ is the inverse image of the fixed point $x_F > \frac{1}{2}$ of the map f . The question now arises how strong the quantity P_{tp} varies if we choose different maps f . Since all doubly symmetric maps are smoothly conjugate to each other we want to study the behaviour of the quantity P_{tp} under conjugation. Let the conjugation u transform the map g into f , i.e. $f = u \circ g \circ u^{-1}$. The invariant measure of g is then given by $\mu_g(x) = \mu_f(u(x))$. It follows that the density transforms according to $\rho_g(x) = \rho_f(u(x)) \frac{du}{dx}$ and we therefore obtain

$$P_{tp} = \int_{u^{-1}(1-x_F)}^1 \rho_g(y) dy \quad (23)$$

The lower integration limit $u^{-1}(1 - x_F)$ can be calculated in the following way. Since $x_F = f(x_F) = u \circ g \circ u^{-1}(x_F)$ we obtain $u^{-1}(x_F) = g(u^{-1}(x_F))$ which means that $u^{-1}(x_F)$ is a fixed point of g . In addition the conjugation u possesses the property $u(x) = 1 - u(1 - x)$ which is due to the fact that we are dealing with symmetric maps. The image of the fixed point x_F of f is therefore also a fixed point of g , i.e. $y_F = u^{-1}(x_F)$ and we arrive at the

final equation

$$P_{tp} = \int_{y_1}^1 \rho_g(y) dy \quad (24)$$

with $y_1 = (1 - y_F)$. This proves the invariance of the statistics of turning points under conjugation. All doubly symmetric maps possess therefore the same ratio of turning points and non turning points and P_{tp} is therefore a universal statistical quantity. Calculating this integral for the specific case of the logistic map yields $P_{tp} = \frac{2}{3}$ which simply means that statistically two out of three points of the trajectories are turning points.

6 Application of the turning point concept to the analysis of one dimensional time series

The above-discussed characteristics of the turning point dynamics in the neighbourhood of the unstable fixed points of the chaotic system can in fact be used to analyze chaotic time series. The main goal of such an analysis is to find the location of the fixed points and higher periodic orbits of the underlying dynamical system.

Since we are interested in fully chaotic and ergodic systems we encounter only hyperbolic fixed points (HFP). We have however to distinguish between HFP with and without reflection. For HFP with reflection subsequent iterations of the map in the vicinity of the fixed point oscillate around the fixed point whereas for HFP without reflection a turning point in the neighbourhood of the fixed point is always followed by a stretching phase away from the fixed point. We will describe below an algorithm which allows us to determine the positions of the fixed points (periodic orbits) of a chaotic time series using these properties. The most important feature of our turning point method for the location of the fixed points is the fact that the above-described properties *are not restricted to the linear neighbourhood of the fixed point*. Therefore the position of the fixed point can be approximately determined even in the case when the linear neighbourhood of the fixed point is not visited by the finite trajectory, i.e. time series, at all.

As a first step of our algorithm we select those points of a given time series $\{x(i)|i = 1, \dots, N\}$ which are turning points, i.e. which obey Eq.(1). The next step distinguishes between HFP with and without reflection. To

determine the HFPs with reflection we select those points $\{x_t(i)\}$ of the turning point trajectory (resulting from the first step) which have as a next iteration point in the original time series also a turning point $\{x_t(i+1)\}$. We group these points according to the values of their center of oscillations defined as $x_{CO}(i) = \frac{1}{2}(x_t(i) + x_t(i+1))$. Thereby points with approximately the same values for $x_{CO}(i)$ belong to the same group. Using the amplitudes of oscillations $d(i) = |x_t(i+1) - x_t(i)|$ we look subsequently within each group for the turning point pair $(\bar{x}_t(i), \bar{x}_t(i+1))$ which corresponds to the minimal amplitude of oscillations. The position of the corresponding HFP is then given by the corresponding center of oscillation $x_F = \frac{1}{2}(\bar{x}_t(i) + \bar{x}_t(i+1))$. By using the minimal amplitude we get rid of the big oscillations which occur due to the effects of the boundaries of the finite interval.

We emphasize that the minimal amplitude of oscillations needs not to be smaller than the size of the linear neighbourhood of the fixed point in order to obtain a good estimation of the position of the fixed point. Our method possesses therefore an advantage compared to methods relying on the properties of the linear regime around the fixed point or recurrence methods. This is due to the fact that the turning around the fixed point is *not* a strongly localized property, and in particular not restricted to the linear regime.

For the HFP without reflection we collect those points of the turning point trajectory which have as subsequent iteration points in the original trajectory non turning points, i.e. points belonging to a stretching phase of motion. If the stretching phase is increasing the value of the coordinate, the corresponding points belong to the group $\{x_t^+(i)\}$ and in the opposite case to $\{x_t^-(i)\}$. As a next step we look for the extrema defined by $x_F^+ = \min\{x_t^+(i)\}$ and $x_F^- = \max\{x_t^-(i)\}$. The position of the fixed point is finally given by $x_F = \frac{1}{2}(x_F^+ + x_F^-)$.

In order to demonstrate the efficiency of our algorithm we have applied it to a time series of the second iterate of the logistic map $f^2(x) = f(f(x))$ with $f(x) = rx(1-x)$ for $r = 3.9$. Using a times series of only 200 points we are able to determine the positions of the fixed points of the system with a relative accuracy of 0.004. For the positions of the two HFP with reflection we get the values $x_{F1} = 0.36052$ and $x_{F2} = 0.89876$ compared to the exact values 0.35897... and 0.89744..., respectively. For the HFP without reflexion we obtain $x_{F3} = 0.74421$ compared to the exact value 0.74359. An analysis of the same time series with, for example, recurrence methods yields a relative accuracy of 0.05 for the position of the fixed points and is therefore much less

accurate. Our algorithm for the turning point analysis of time series yields reliable results even if the number of points of the time series is comparatively small.

The above algorithm can also be applied to the case of a scalar experimental 1D time series, i.e. a chaotic signal, which originates from a higher dimensional dynamics. It is therefore by no means restricted to a 1D time series arising from a 1D system. The oscillating behaviour around the unstable fixed points described above represent a characteristic feature of each component of a multidimensional signal. Indeed the chaotic dynamics of a multidimensional system in the neighbourhood of a fixed point can be characterized by the fact that the deflection or turning of the different trajectories approaching the fixed point varies significantly and therefore turnings can occur with respect to any direction of space. As examples for two-dimensional fully chaotic systems we mention the Ikeda [Ikeda,1979] or Henon map [Henon,1976] which exhibits oscillatory behaviour with small amplitudes around the position of the fixed point for both components x as well as y .

7 Summary and Outlook

We have investigated the ergodic and fully developed chaotic behaviour of SSH maps in some detail. Our starting point was the observation that the chaotic trajectories suggest the existence of certain nontrivial structures around the unstable fixed point. A closer look at the trajectories showed us that these structures have their origin in the distribution of oscillations in the unit interval. A comparison of the densities for the center of oscillations as well as their amplitudes with the corresponding quantities for a weighted random map clearly revealed that the dynamics of the oscillations is highly organized and far from being random. Characteristics of the amplitude of oscillations as a function of the center of oscillations have been discussed.

The central idea of our investigation is the introduction of a turning point analysis as a tool for the characterization of the dynamics of ergodic and fully developed chaotic systems. On our way of a quantification of this idea we have derived a turning point criterion which gives us a condition for the point $x(n-1)$ so that $x(n)$ becomes a turning point. With the help of this criterion we were able to understand the dynamics of turning points. Roughly speaking the trajectories possess two phases of motion: a stretching

phase in the neighbourhood of the unstable fixed point 0 which consists apart from its important first point only of non turning points and an oscillating stretching phase around the second unstable fixed point x_F which consists exclusively of turning points.

As an important tool we have subsequently introduced the turning point map (TPM) which illustrates the mapping of successive turning points. This TPM exhibits a number of dynamically interesting properties. It contains details of the first hump of iterates f^i for all i and maps in particular arbitrarily small intervals in the neighbourhood of the origin onto the finite interval $[x_F, 1]$. The TPM obeys an asymptotic scaling law and converges to a repeating functional form. A construction scheme for the humps in the asymptotic scaling regime has been derived. Another important property of the TPM is the fact that it allows us to locate the fixed point x_F as well as all its preimages. The turning point dynamics shows an infinite correlation length of the corresponding correlation function, i.e. the turning point analysis extracts the correlated part from the originally completely uncorrelated trajectory. The origin of this strong correlation is the oscillating dynamics around the fixed point x_F .

We have shown that it is possible to define a so-called renormalized limit function which corresponds to the renormalized version of the infinitely iterated map. The renormalization is performed with respect to successive zeros. Successive humps are scaled onto the unit interval. We have illustrated the construction scheme of the limit function for the example of the logistic map.

As a next step we have investigated the TPMs belonging to higher iterates of the original map f . The TPMs themselves as well as their disconnected constituents show an asymptotic scaling behaviour and exactly describe important parts of arbitrarily high iterates of the map f . It is possible to extract the position of not too long periodic orbits of f by considering the TPM of the corresponding iterate f^n . A limited amount of information on the stability of the periodic orbits can be obtained from the scaling laws of the constituents of the TPMs. Informations on the position of high preimages of the fixed points can easily be extracted.

We have performed a statistical analysis of the turning point dynamics for the special case of doubly symmetric maps. We could show that the ratio of turning points to the total number of points is an invariant for these maps and takes on the value $\frac{2}{3}$. This suggests that the ratio might be used for a characterization of nonsymmetric maps and divides the maps into different

equivalence classes.

Our investigation and discussion of the dynamical and statistical behaviour of the turning points, the TPMs as well as the correlation functions clearly show that a turning point analysis extracts valuable information from a given ergodic and fully chaotic system and is very well-suited for the analysis of chaotic time series. Using the main features of the dynamics of the turning points in the neighbourhood of the fixed point we developed an algorithm which allows us to locate the unstable fixed points and higher periodic orbits thereby distinguishing between hyperbolic fixed points with and without reflection. The most important property of our turning point method for the location of the fixed points is the fact that it is not restricted to the linear neighbourhood of the fixed point. Even in the case when the linear regime around the fixed point is not visited by the time series at all, it is possible to determine approximately the position of the fixed point. Our turning point analysis of the time series yields reliable results in particular if the number of points of the time series is comparatively small and represents therefore an attractive method for the investigation of dynamical systems of, for example, biological origin.

Acknowledgements

The European Community (F.K.D.) is gratefully acknowledged for financial support.

References

F.T.Arecchi, R.Meucci, G.Puccioni and J.Tredicce [1982], "Experimental evidence of subharmonic bifurcations, multistability, and turbulence in a Q-switched gas laser", Phys.Rev.Lett.**49**, 1217-1220

C.Beck and F.Schlögl [1993], "Thermodynamics of chaotic systems", Cambridge Nonlinear Science Series.

A.Blokh and M.Misiurewicz, "*New order for periodic orbits of interval maps*", preprint

P.Collet and J.P.Eckmann [1980], "Iterated maps on the interval as dynamical systems", Birkhäuser, Cambridge Massachusetts

J.P.Crutchfield, J.D.Farmer and B.A.Huberman [1982], "Fluctuations and simple chaotic dynamics", Phys.Rep.**92**, 45-82

F.K.Diakonov and P.Schmelcher [1997], subm.to CHAOS

F.K.Diakonov and P.Schmelcher [1996], "On the construction of one-dimensional iterative maps from the invariant density: the dynamical route to the beta distribution", Phys.Lett.A**211**, 199

F.K.Diakonov and P.Schmelcher, in preparation

E.J.Ding [1988], "Wave numbers for unimodal maps", Phys.Rev.A**37**, 1827-1830

M.Feigenbaum [1978], "Quantitative universality for a class of nonlinear transformations", J.Stat.Phys.**19**, 25-52

M.Feigenbaum [1979], "The universal metric properties of nonlinear transformations", J.Stat.Phys.**21**, 669-706

J.P.Gollub and S.V.Benson [1980], "Many routes to turbulent convection", J.Fluid Mech.**100**, 449-470

S.Grossmann and S.Thomae [1977], "Invariant distributions and stationary correlation functions of one-dimensional discrete processes", Zeitschrift für Naturforschung **32**, 1353-1363

G.Györgyi and P.Szepfalusy [1984], "Fully developed chaotic 1-d maps", Z.Phys.B**55**, 179-186

G.Györgyi and P.Szepfalusy [1984], "Properties of fully developed chaos in one-dimensional maps", J.Stat.Phys.**34**, 451-475

M.Henon [1976], "A Two-dimensional Mapping with a Strange Attractor", Comm.math. Phys.**50**, 69-77

K.Ikeda [1979], "Multiple-valued stationary state and its instability of the transmitted light by a ring cavity system", Opt. Comm. **30**, 257

L.Kadanoff [1983], "Roads to chaos", Physics Today, p.46-53

P.S.Linsay [1981], "Period doubling and chaotic behavior in a driven anharmonic oscillator", Phys.Rev.Lett.**47**, 1349-1352

E.Ott [1993], "Chaos in dynamical systems", Cambridge Univ. Press, Cambridge

S.Pincherle [1920], "On the complete iteration of $x^2 - 2$ ", Rend. della Real Acad. dei Lincei **29**, 329-333

R.Z.Sagdeev, D.A.Usikov and G.M.Zaslavsky [1990], "Nonlinear Physics", Harwood Academic Publishers, New York

H.G.Schuster [1994], "Deterministic Chaos", VCH Weinheim

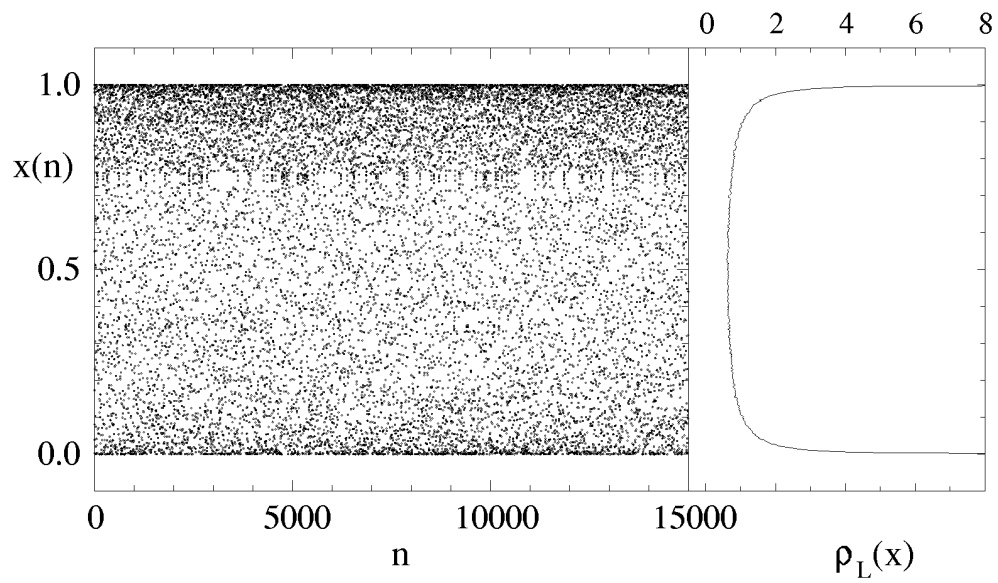


Figure 1: A chaotic and ergodic trajectory $x(n)$ of the logistic map for 1.5×10^4 iterations and the invariant density ρ_L of the same trajectory for 10^6 iterations.

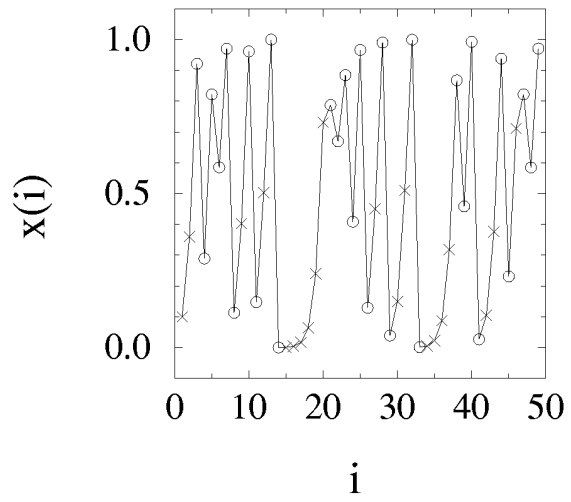


Figure 2: 50 iterations of a trajectory of the logistic map. The turning points are indicated with circles whereas the non-turning points are indicated with crosses. The stretching and oscillatory phases of motion are clearly visible.

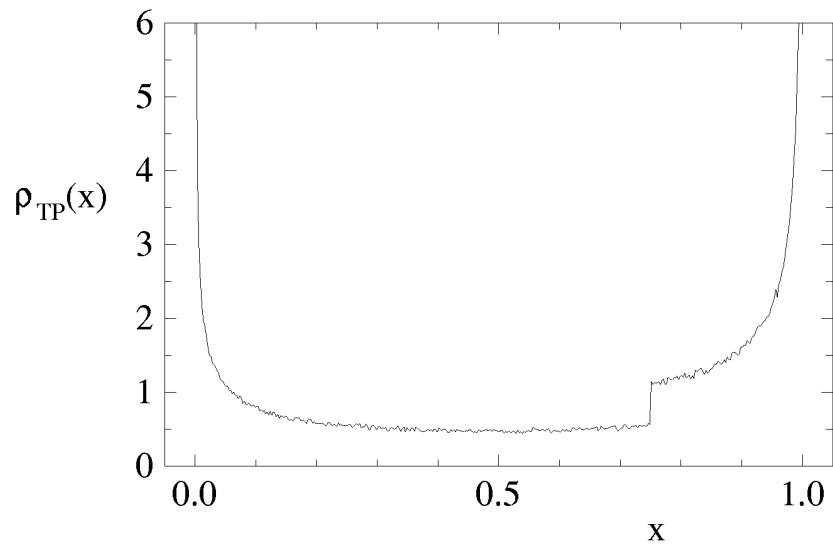


Figure 3: The turning point density ρ_{TP} of the logistic map. The step like structure is at the position of the fixed point x_F .

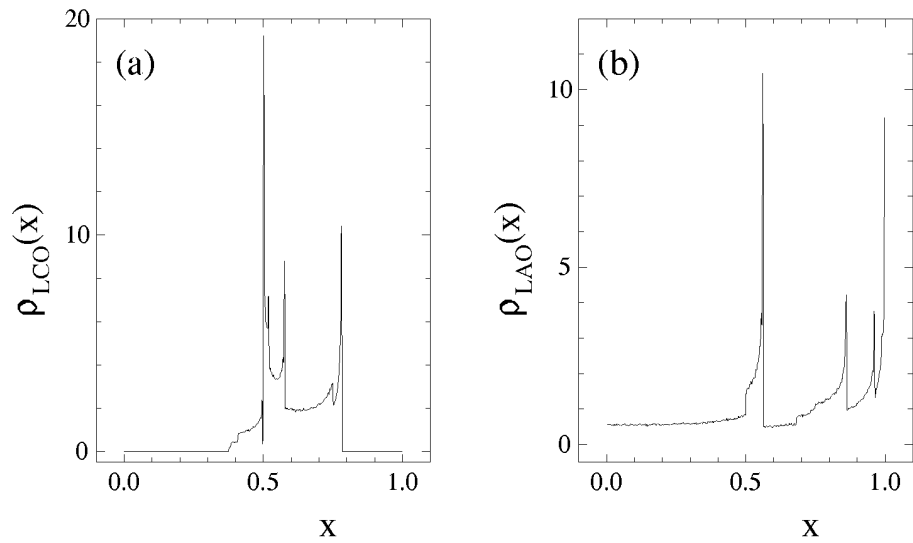


Figure 4: (a) The density for the centers of the oscillations $\rho_{LCO}(x)$ of a typical chaotic trajectory of the logistic map. (b) The density for the amplitudes of the oscillations $\rho_{LAO}(x)$ of the same trajectory.

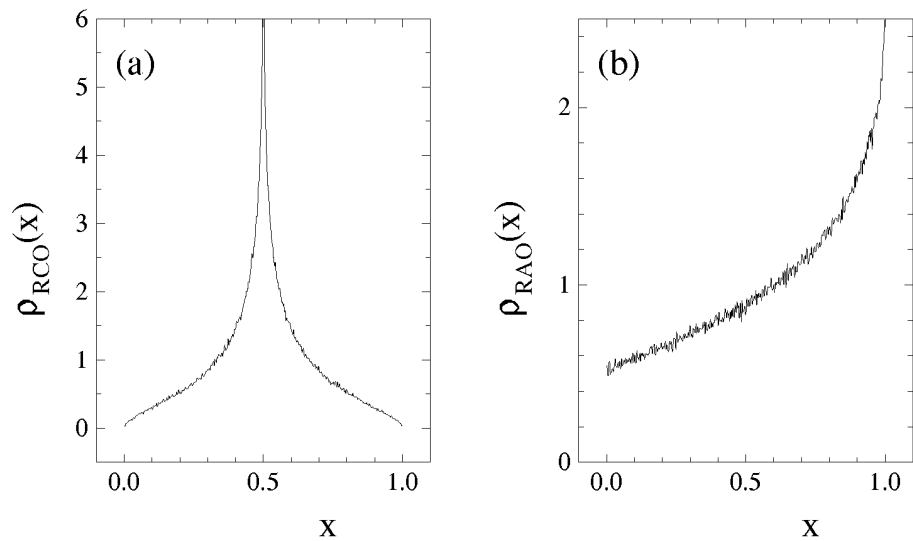


Figure 5: (a) The density for the centers of the oscillations $\rho_{RCO}(x)$ of a trajectory of the weighted random map with $\rho_R = \rho_L$. (b) The density for the amplitudes of the oscillations $\rho_{RAO}(x)$ of the same trajectory.

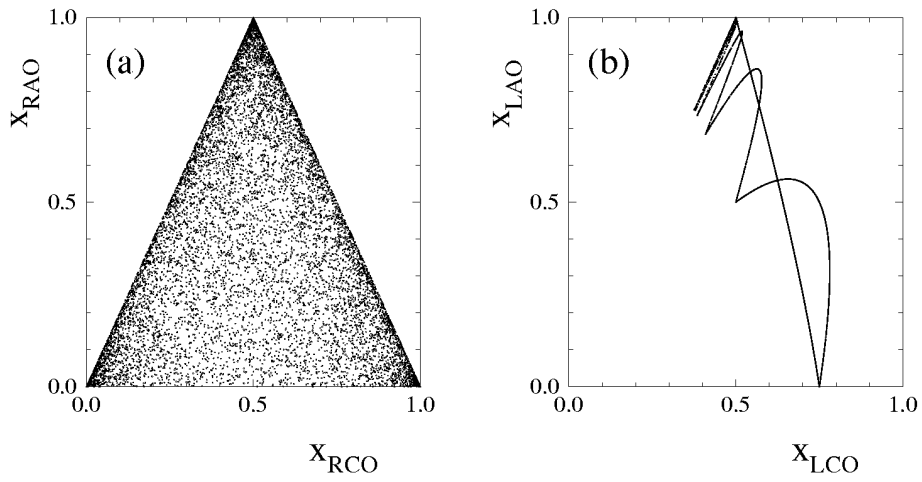


Figure 6: (a) The amplitudes of the oscillations as a function of the centers of the oscillations $x_{RAO}(x_{RCO})$ for the random map. (b) The amplitudes of the oscillations as a function of the centers of the oscillations $x_{LAO}(x_{LCO})$ for the logistic map.

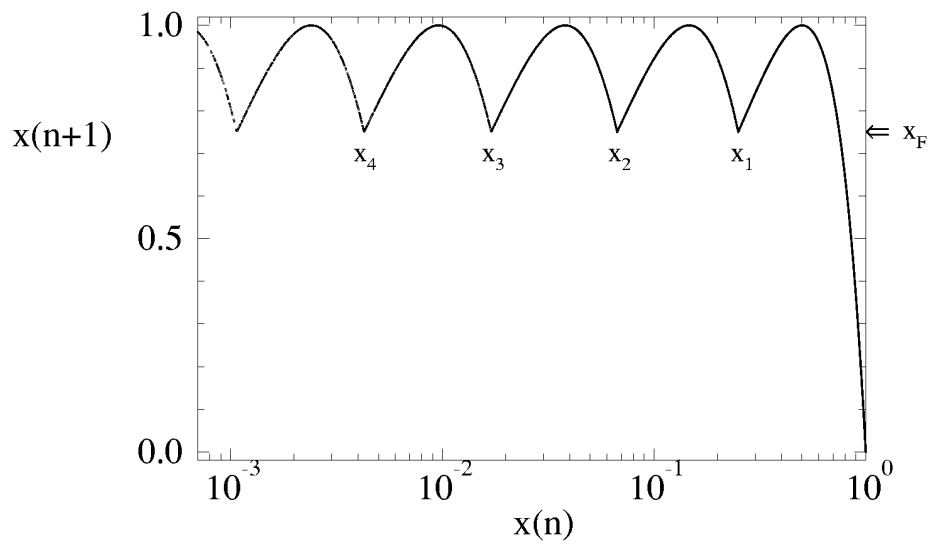


Figure 7: The turning point map of the logistic map for a logarithmic abscissae. x_i are successive preimages of the unstable fixed point $x_F = \frac{3}{4}$ on the left branch of f .

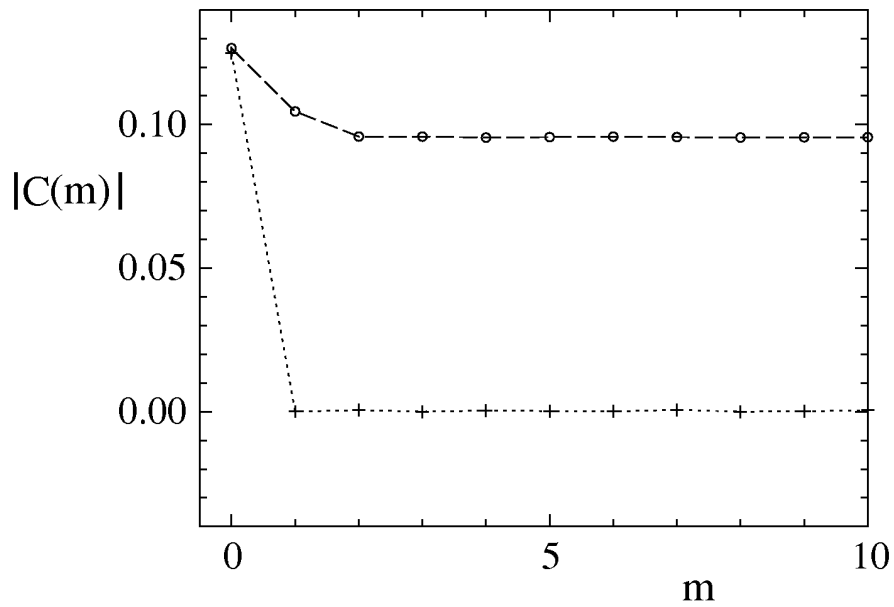


Figure 8: The absolute value $|C(m)|$ of the correlation function $C(m) = \langle (x - \langle x \rangle_f)(f^m(x) - \langle x \rangle_f) \rangle_f$ for the logistic map. Circles indicate the correlation function of the turning points and crosses the correlation function of the original trajectory.

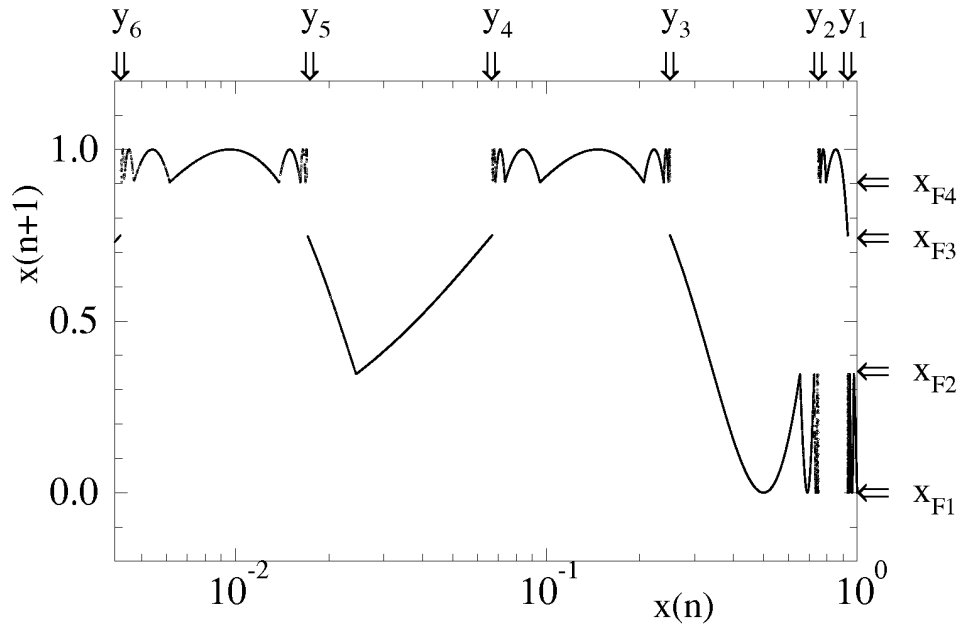


Figure 9: The turning point map of the doubly iterated logistic map f^2 for a logarithmic abscissae. The disconnected objects (a), (e) repeat themselves in an asymptotically scaling way if we approach the unstable fixed point 0. All objects show also an interior scaling behaviour (see Figure 9). y_i correspond to the positions of the preimages of the fixed point with a positive derivative, i.e. preimages of $x_{F3} = \frac{3}{4}$. The positions of the fixed points x_{F_i} of f^2 are indicated on the vertical axis.

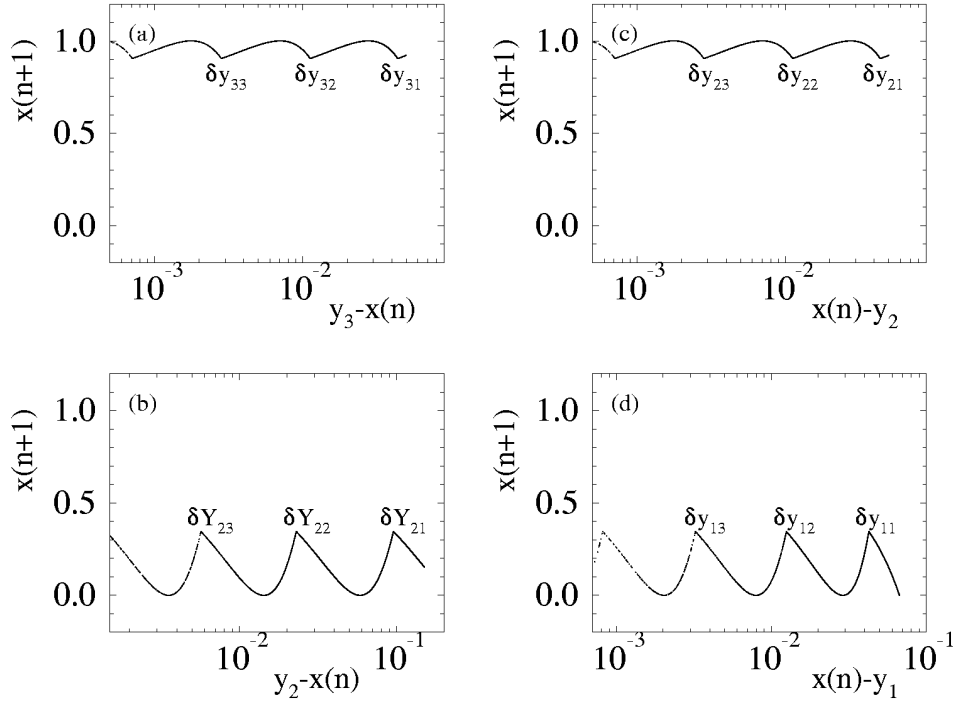


Figure 10: Magnified parts of the objects (a), (b), (c), (d) of Figure 8 are shown on a logarithmic scale. The scaling behaviour of the interior of these objects becomes evident. (a) Scaling behaviour towards the preimage y_3 of x_{F3} by a series $\delta y_{31}, \delta y_{32}, \delta y_{33}, \dots$ of preimages of the fixed point x_{F4} . (b) Scaling behaviour towards the preimage y_2 of x_{F3} by a series $\delta Y_{21}, \delta Y_{22}, \delta Y_{23}, \dots$ of preimages of the fixed point x_{F2} . (c) Scaling behaviour towards the preimage y_2 of x_{F3} by a series $\delta y_{21}, \delta y_{22}, \delta y_{23}, \dots$ of preimages of the fixed point x_{F4} . (d) Scaling behaviour towards the preimage y_1 of x_{F3} by a series $\delta y_{11}, \delta y_{12}, \delta y_{13}, \dots$ of preimages of the fixed point x_{F2} .

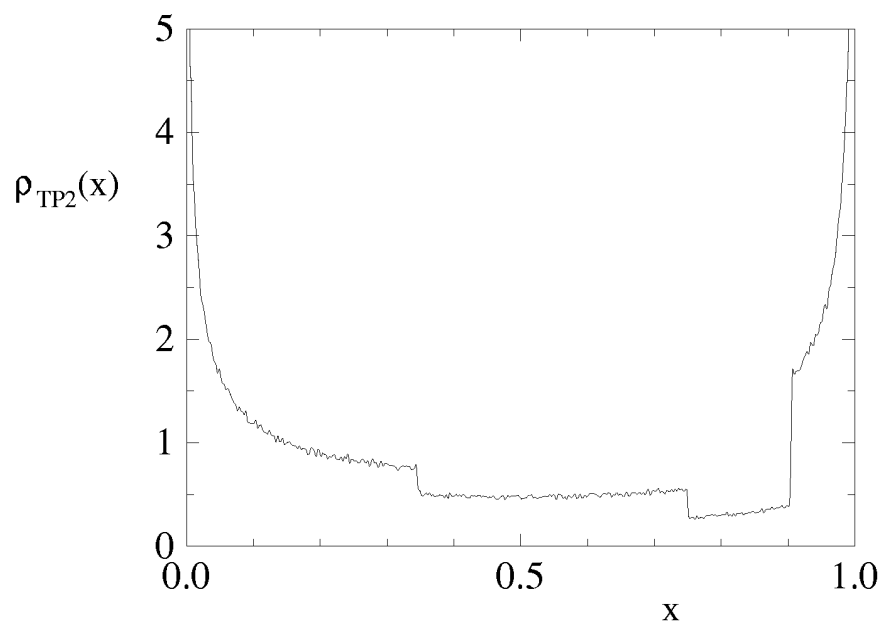


Figure 11: The density ρ_{TP2} of the turning points of the doubly iterated logistic map f^2 . Three step like structure are clearly visible. The positions of these steps are the fixed points x_{Fi} of f^2 .